Pharmacogenetics-Based Population Pharmacokinetic Analysis of Efavirenz in HIV-1-Infected Individuals

M Arab-Alameddine[1,2], J Di Iulio[3], T Buclin[1], M Rotger[3], R Lubomirov[3], M Cavassini[4], A Fayet[1], LA Décosterd[1], CB Eap[5], J Biollaz[1], A Telenti[3] and C Csajka[1,2]; the Swiss HIV Cohort Study

Besides CYP2B6, other polymorphic enzymes contribute to efavirenz (EFV) interindividual variability. This study was aimed at quantifying the impact of multiple alleles on EFV disposition. Plasma samples from 169 human immunodeficiency virus (HIV) patients characterized for *CYP2B6, CYP2A6*, and *CYP3A4/5* allelic diversity were used to build up a population pharmacokinetic model using NONMEM (non-linear mixed effects modeling), the aim being to seek a general approach combining genetic and demographic covariates. Average clearance (CL) was 11.3 l/h with a 65% interindividual variability that was explained largely by *CYP2B6* genetic variation (31%). *CYP2A6* and *CYP3A4* had a prominent influence on CL, mostly when *CYP2B6* was impaired. Pharmacogenetics fully accounted for ethnicity, leaving body weight as the only significant demographic factor influencing CL. Square roots of the numbers of functional alleles best described the influence of each gene, without interaction. Functional genetic variations in both principal and accessory metabolic pathways demonstrate a joint impact on EFV disposition. Therefore, dosage adjustment in accordance with the type of polymorphism (*CYP2B6*, *CYP2A6*, or *CYP3A4*) is required in order to maintain EFV within the therapeutic target levels.

Efavirenz (EFV), a non-nucleoside reverse transcriptase inhibitor, is widely used in combination with nucleoside inhibitors as first-line treatment of type I human immunodeficiency virus (HIV-1) infection. It is generally prescribed at a fixed dosage of 600 mg daily, despite the presence of a marked interindividual variability in tendency to produce elevated plasma drug concentration levels[1–3] that have been shown to be associated with central nervous system toxicity.[4–6]

EFV is metabolized primarily by *CYP2B6* and, to a lesser extent, by accessory pathways involving *CYP2A6*, *CYP3A4/3A5*, and uridine-glucuronyl-transferases.[7–9] Several studies have shown that *CYP2B6* is highly polymorphic and that genetic variations play an important part in EFV plasma concentration variability.[5,10–15] Genetic polymorphisms of *CYP3A4/3A5* have also been associated with higher EFV exposure,[6] but the influence of the *CYP2A6* polymorphism on EFV pharmacokinetics has not yet been characterized. Considering the increasing number of allelic variants that are being described and the resulting complexity of allele combinations that could influence EFV elimination, we conducted a population pharmacokinetic analysis in HIV-1-infected individuals fully characterized for *CYP2B6*, *CYP2A6*, and *CYP3A4/A5* genetic variations. Our main areas of focus were: (i) to assess the relative contributions of multiple functional alleles involved in EFV elimination along with other demographic or environmental factors, (ii) to characterize the nature of the relationship between individual allelic constitution and EFV disposition, and (iii) to explore models for gene–gene interactions that could lead to a better understanding of the interrelationships of specific enzymes involved in EFV elimination.

RESULTS

In total, 393 plasma samples were collected from 169 individuals. Concentration measurements ranged between 100 and 59,400 ng/ml. A one-compartment model with first-order absorption from the gastrointestinal tract fitted the data

The first two authors contributed equally to this work.
[1]Division of Clinical Pharmacology and Toxicology, University Hospital Center, University of Lausanne, Lausanne, Switzerland; [2]Department of Pharmaceutical Sciences, Clinical Pharmacy Unit, University of Geneva, Geneva, Switzerland; [3]Institute of Microbiology, University Hospital Center, University of Lausanne, Lausanne, Switzerland; [4]Division of Infectious Diseases, University Hospital Center, University of Lausanne, Lausanne, Switzerland; [5]Unit of Biochemistry, Cery Hospital, University of Lausanne, Lausanne, Switzerland. Correspondence: C Csajka (chantal.csajka@chuv.ch)

Received 28 August 2008; accepted 1 December 2008; advance online publication 18 February 2009. doi:10.1038/clpt.2008.271

appropriately. Average clearance (CL) was 11.3 l/h with an interindividual variability of 65%, the volume of distribution (V) was 388 l, and the absorption constant (k_a) was 0.62 h^{-1}. The assignment of interindividual variability on either V or k_a did not improve the fit (change in objective function (ΔOF) = 0.0).

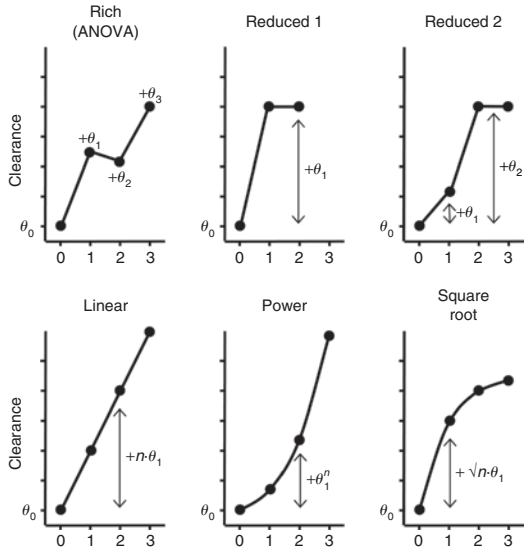

Figure 1 Various parameter models were tested to describe the level of oral clearance (*Y*-axis) as a function of the number of functional alleles of an enzyme (*X*-axis): 0 = Hom-LOF, 1 = Het-LOF, 2 = Hom-Ref, 3 = Het-GOF (a specific parameter for Het-GOF, is required only with *CYP2B6*). ANOVA, analysis of variance; GOF, gain of function; Het, heterozygous; Hom, homozygous; LOF, loss of function; Ref, reference allele.

Demographic analyses

Body weight and black ethnicity influenced CL, as did gender, age and, to a lesser extent, height. Co-medications were shown to have no significant influence on EFV pharmacokinetics. A multivariable combination of demographic factors revealed that body weight accounted for the effect of height, age, and gender while explaining 3% of CL variability, and it was the only demographic factor influencing CL besides black ethnicity, which remained statistically significant beyond body weight and reduced the variability in CL by another 3%.

Univariate genotype analyses

The influence of *CYP2B6*, *CYP2A6*, *CYP3A4/AA5* functional alleles on EFV CL was first tested in single-gene analyses, in which the allelic variants (Hom-LOF, Het-LOF, and Hom-Ref plus Het-GOF for *CYP2B6*) were entered into the model as covariates that partitioned individuals based on their genetic constitution.

Genetic variation of *CYP2B6* had by far the most salient impact on CL. Several competing models were tested, as depicted in Figure 1. The richest possible model, which assigned a separate fixed effect to each of the *CYP2B6* allelic variants (Eqs. 1/1a), markedly improved the fit and explained 31% of the 65% interindividual variability on CL. The average CL was 2.8 l/h in the Hom-LOF group and 10.8, 13.3, and 18.8 l/h in individuals carrying Het-LOF, Hom-Ref, and Het-GOF alleles, respectively. A series of reduced models showed CL to be statistically different among all *CYP2B6* groups (ΔOF = +9 and ΔOF = +10 for model reduced 1 and 2). Competing simplified models were tried to

Table 1 Functional alleles evaluated in the study and genotype-based activity score classification

Functional alleles					
Functional consequence	**CYP2B6 alleles**	**CYP2A6 alleles**	**CYP3A4 alleles**	**CYP3A5 alleles**	
Loss of function (LOF)	*11, *15, *28	*2, *4		*3, *6, *7, *10, *11	
Diminished function (DOF)	*6, *18, *27, *29	*1H, *1J, *5, *7, *9, *10, *12, *13, *15, *17, *19, *34	rs4646437 *1B	—	
>25%		*5, *7, *9, *10, *12, *13, *15, *17, *19, *34	—	—	
<25%		*1H, *1J	—	—	
Reference	*1, *2, *3, *5, *17	*1	*1	*1	
Gain of function (GOF)	*4, *22	*1X2	—	—	
Genotypes and activity score classification					
Score A	**Alleles (allele 1/allele 2)**	**Score B**	**Alleles (allele 1/allele 2)**	**Score C***	**Alleles (allele 1/allele 2)**
0	LOF/LOF LOF/DOF DOF/DOF	0	LOF/LOF	0	LOF/LOF
1	Ref/LOF Ref/DOF	0.25	LOF/DOF	0.25	LOF/DOF
2	Ref/Ref	0.5	Ref/LOF DOF/DOF	0.5	Ref/LOF
3	Ref/GOF	1	Ref/LOF	0.75	DOF/DOF
		1.5	Ref/DOF	1	Ref/DOF >25%
		2	Ref/Ref	1.5	Ref/DOF <25%
				2	Ref/Ref

DOF, diminished function; GOF, gain of function; LOF, loss of function; Ref, reference allele.

*Only for CYP2A6 alleles.

estimate CL as a function of the number of functional alleles, as defined by the activity score A (**Table 1**) and were compared with the richest model (Eqs. 1/1a); the use of a linear model (Eq. 2) or a power function model (Eq. 3) did not fit the data appropriately (ΔOF = +18.5 and +58.8, respectively). As interim explorations showed CL to be modestly reduced by ~25% in Het-LOF carriers but cut down by 75% in Hom-LOF individuals, a square root function model achieved the best fit using either an additive (Eq. 4) or a proportional model (ΔOF = −167.7). The recourse to alternative activity scores B for *CYP2B6*, allowing for the distinction between loss and decrease of function alleles, did not better characterize the genotype–phenotype relationships using Eq. 2, 3, or 4 (ΔOF >+8.2).

The assignment of *CYP2A6* allelic variants on CL using the richest model (Eqs. 1/1a) improved the fits (ΔOF = −7.9) and decreased by 1% the overall variability on CL. The average CL was 7.0, 10.8, and 12.1 l/h in Hom-LOF, Het-LOF, and Hom-Ref individuals, respectively. The difference in CL between Hom-Ref and Het-LOF individuals was not significant (ΔOF = −1.0). The description of the relationship between CL and the functional score, using either linear (Eq. 2) or power (Eq. 3) models, did not fit the data adequately when compared with the richest model (ΔOF >+6.8), whereas it was again best characterized using a square root function (Eq. 4) that provided a fit almost identical to that of the rich model (ΔOF = −7.8). Here too, the model integrating partial activity levels (scores B/C) did not improve data description (ΔOF = −0.4 for score B and −0.1 for score C).

The impact of *CYP3A4* on EFV CL was tested using two alleles associated with changes in function, *CYP3A4*1B* and *CYP3A4_* rs4646437. The rich model (Eqs. 1/1a) showed that both alleles influenced CL to a significant extent (ΔOF = −25.4 for *CYP3A4_* rs4646437, −10.4 for *CYP3A4*1B*). CL in Hom-LOF, Het-LOF, and Hom-Ref carriers were, respectively, 5.1, 10.3, and 11.9 l/h for *CYP3A4*1B* and 3.7, 10.7, and 12.3 l/h for *CYP3A4_* rs4646437 alleles. After inclusion of *CYP3A4*1B* and *CYP3A4_* rs4646437 alleles in the model, interindividual variability in CL dropped from 65 to 62 and 59%, respectively. The differences in CL between Hom-Ref and Het-LOF individuals were not significant, both for **1B* and for rs4646437 (ΔOF = −1.4 for *CYP3A4_* rs4646437 and −0.9 for *CYP3A4*1B*). When compared with the richest model, linear and power function models (Eqs. 2/3) did not fit the data adequately (ΔOF >+8.0); square root models (Eq. 4) described the data best (ΔOF = −10.3 for *CYP3A4*1B* and −24.8 for *CYP3A4_* rs4646437).

The influence of *CYP3A5* functional alleles on CL was shown to be small but significant, using the rich model (Eqs. 1/1a, ΔOF = −8.1), with a residual 64% interindividual variability. The difference in CL between individuals with Het-LOF allele and those with Hom-Ref allele was not significant (ΔOF = −0.0). None of the above models (Eqs. 2/3) could characterize the relationship between CL and *CYP3A5* allele variants better than the square root model could (Eq. 4, ΔOF = −8.2).

The effect of black ethnicity remained a statistically influencing covariate on CL in addition to genetic variation, causing an additional 25–40% decrease in CL when associated with functional alleles (ΔOF compared to *CYP2B6* = −8.1, *CYP2A6* = −9.9, *CYP3A4*1B* = −4.0, and *CYP3A5* = −7.8), except for *CYP3A4_* rs4646437 (ΔOF = −0.4), which was present in most of the black individuals, thus limiting the power to detect any association.

Gene–gene interaction analyses

The joint influence of functional alleles on EFV CL was first tested through the conjunction of *CYP2B6* with each of the other *CYP* alleles in dual-gene models, to finally build up the model including all genetic variables having influence on CL. The richest model (Eq. 5) characterizing the joint influence of *CYP2B6* and *CYP2A6*, using a fixed effect parameter for each allelic combination, suggested an additional contribution of *CYP2A6* in EFV elimination (ΔOF = −20 as compared to the final model for *CYP2B6*, Eq. 4). Competitive models were developed based on a functional score A (**Table 1**) using square root function models. The models evaluating the contribution of *CYP2A6* variation, whether on each *CYP2B6* genotypic group separately (Eq. 6) or through the use of a single parameter estimate across all *CYP2B6* allelic variants (Eq. 7), fitted the data with similar adequacy (ΔOF >−16), resulting in an absolute increase in CL of 1.2 and 1.7 l/h in *CYP2A6* Het-LOF and Hom-Ref individuals, respectively, as compared to Hom-LOF carriers. The contribution of *CYP2A6* functional alleles was more prominent in *CYP2B6* Hom-LOF carriers, in whom the relative change in CL was estimated to be 44% per active allele as compared to an 11% change in Hom-Ref individuals. The joint gene influence could be further described by simply adding *CYP2B6* and *CYP2A6* square root functions (Eq. 8, ΔOF = −12). This model was not considered statistically different from previous models (Eqs. 6/7), considering the reduced degrees of freedom and the loss of fit from the richest possible model (Eq. 5, ΔOF = +8). The introduction of a single interaction factor (Eq. 9) to evaluate some hyper- or hypo-additive trend did not produce any significant change (ΔOF = +3).

The same paradigm was successfully applied to characterize the other gene–gene interactions. The rich model (Eq. 5) characterizing the joint influence of *CYP2B6* with the *CYP3A4*1B* or *CYP3A4* rs4646437 alleles suggested an additive effect of both genes on EFV CL (ΔOF = −14 for **1B*, −25 for rs4646437). Reduced models integrating square root functions of *CYP3A4* activity scores on *CYP2B6* stratified by allelic variation (Eq. 6) described the data appropriately (ΔOF = −13 for **1B,* −18 for rs_4646437), and no deterioration of the fit was observed when allowing a single parameter estimate (Eq. 7) for the effect of *CYP3A4* across all *CYP2B6* allelic variants (ΔOF = +1.0 for **1B,* 0.0 for rs_4646437 as compared to Eq. 6). The additive contribution of *CYP3A4* on CL was 1.1 and 1.5 l/h in **1B* Het-LOF and Hom-Ref carriers, respectively, and 1.4 and 1.9 l/h in rs_4646437 Het-LOF and Hom-Ref carriers, respectively. CL increased by 40 (**1B*) and 48% (rs_4646437) per active allele of *CYP2B6* and *CYP3A4* as compared to the respective Hom-LOF. Further characterization of the joint contribution of *CYP2B6* and *CYP3A4* on EFV CL, using a mere addition of square root functions (Eq. 8), fitted the data appropriately, the loss of fit in comparison with previous models (Eqs. 5/6/7) being not significant (ΔOF = −9.0

Table 2 Summary of the key models used to examine the influence of demographic and genetic covariates on EFV clearance

Step 1	Demographic model	Model	θ_0	θ_1	θ_2	θ_3	ΔOF	*P*
	Body weight (BW)	$CL = \theta_0 \cdot (1 + \theta_1 \cdot BW)$	11.5	1.2			−25.6	**
	Height	$CL = \theta_0 \cdot (1 + \theta_1 \cdot Hgt)$	11.2	2.3			−4.2	*
	Age	$CL = \theta_0 \cdot (1 + \theta_1 \cdot age)$	12	0.7			−5.7	*
	Sex (M = 0, F = 1)	$CL = \theta_0 \cdot (1 + \theta_1 \cdot sex)$	12	0.2			−4.1	*
	Race	$CL = \theta_0(1 - q) + \theta_1 \cdot q$						
	Black (q = 1) vs. others (q = 0)		11.8	6.25			−13.2	**
	White (q = 1) vs. others (q = 0)		12	7.1			−7.7	**
	Hispanic (q = 1) vs. others (q = 0)		15.1	11.2			−0.9	NS
	Asian (q = 1) vs. others (q = 0)		11.3	9.8			−0.13	NS
	Other ARV							
	Ritonavir (RTV)	$\theta_0 \cdot (1 + \theta_1 \cdot RTV)$	11.3	0.01			0.2	NS
	Zidovudine (AZT)	$\theta_0 \cdot (1 + \theta_1 \cdot AZT)$	10.4	0.12			−1.1	NS
	Lamivudine	$\theta_0 \cdot (1 + \theta_1 \cdot 3TC)$	10.6	0.09			−0.6	NS
	NRTI in general	$\theta_0 \cdot (1 + \theta_1 \cdot NRTI)$	8.6	0.3			−1.8	NS
	PI in general	$\theta_0 \cdot (1 + \theta_1 \cdot PI)$	11.3	0.01			0.6	NS
Step 2	**Genotype-variant analysis**	**Model**	**CL_0**	**θ_1**	**θ_2**	**θ_3**	**ΔOF**	***P***
CYP2B6								
Rich: Eq. 1	I_1: Het-LOF, I_2: Hom-Ref, I_3: GOF	$CL = CL_0 + \theta_1 I_1 + \theta_2 I_2 + \theta_3 I_3$	2.8	10.8	13.3	18.8	−171	**
Reduced 1	I_1: Het-LOF or Hom-Ref, I_3: GOF	$CL = CL_0 + \theta_1 I_1 + \theta_3 I_3$	2.8	12.2	—	18.9	−162	**,[a]
Reduced 2	I_1: Het-LOF, I_2: Hom-Ref or GOF	$CL = CL_0 + \theta_1 I_1 + \theta_2 I_2$	2.8	10.8	14.2		−161	**,[a]
Eq. 2	n = 0, 1, 2, 3	$CL = CL_0 + \theta_1 \cdot n$	3.11	5.99			−152	**,[a]
Eq. 3		$CL = CL_0 + \theta_1^n$	5.03	2.9			−76	**,[a]
Eq. 4		$CL = CL_0 + \theta_1 \cdot \sqrt{n}$	2.8	7.8			−168	NS[a]
CYP2A6								
Rich: Eq. 1	I_1: Het-LOF, I_2: Hom-Ref	$CL = CL_0 + \theta_1 I_1 + \theta_2 I_2$	7.0	10.8	12.1		−7.9	*
Reduced 1	I_1: Het-LOF or Hom-Ref	$CL = CL_0 + \theta_1 I_1$	7.0	11.7			−6.9	NS[a]
Eq. 2	n = 0, 1, 2	$CL = CL_0 + \theta_1 \cdot n$	7.75	2.31			−6.8	NS[a]
Eq. 3		$CL = CL_0 + \theta_1^n$	7.8	2.11			−5.3	NS[a]
Eq. 4		$CL = CL_0 + \theta_1 \cdot \sqrt{n}$	7.0	3.63			−7.8	NS[a]
CYP3A4 rs4646437								
Rich: Eq. 1	I_1: Het-LOF, I_2: Hom-Ref	$CL = CL_0 + \theta_1 I_1 + \theta_2 I_2$	3.7	10.7	12.3		−25.4	**
Reduced 1 Eq. 1	I_1: Het-LOF or Hom-Ref	$CL = CL_0 + \theta_1 I_1$	3.7	11.9			−24	NS[a]
Eq. 2	n = 0, 1, 2	$CL = CL_0 + \theta_1 \cdot n$	4.84	4.06			−20	*,[a]
Eq. 3		$CL = CL_0 + \theta_1^n$	6.2	2.5			−12.9	*,[a]
Eq. 4		$CL = CL_0 + \theta_1 \cdot \sqrt{n}$	3.89	6.1			−24.8	NS[a]
*CYP3A4*1B*								
Rich: Eq. 1	I_1: Het-LOF, I_2: Hom-Ref	$CL = CL_0 + \theta_1 I_1 + \theta_2 I_2$	5.1	10.3	11.9		−10.4	**
Reduced 1 Eq. 1	I_1: Het-LOF or Hom-Ref	$CL = CL_0 + \theta_1 I_1$	5.1	11.7			−9.5	NS[a]
Eq. 2	n = 0, 1, 2	$CL = CL_0 + \theta_1 \cdot n$	6	3.6			−9.0	NS[a]
Eq. 3		$CL = CL_0 + \theta_1^n$	6.4	2.3			−7.0	NS[a]
Eq. 4		$CL = CL_0 + \theta_1 \cdot \sqrt{n}$	5.2	4.8			−10.4	NS[a]
CYP3A5								
Rich: Eq. 1	I_1: Het-LOF, I_2: Hom-LOF	$CL = CL_0 + \theta_1 I_1 + \theta_2 I_2$	4.4	10.3	11.8		−8.4	**
Reduced 1 Eq. 1	I_1: Het-LOF or Hom-LOF	$CL = CL_0 + \theta_1 I_1$	4.4	11.5			−7.4	NS[a]
Eq. 2	n = 0, 1, 2	$CL = CL_0 + \theta_1 \cdot n$	6.15	2.96			−6.4	NS[a]
Eq. 3		$CL = CL_0 + \theta_1^n$	7.0	2.22			−4.8	*,[a]
Eq. 4		$CL = CL_0 + \theta_1 \cdot \sqrt{n}$	4.7	5.2			−8.1	NS[a]

Table 2 Continued on next page

Table 2 (Continued)

Step 3	Gene–gene interaction analysis	*CYP* contribution	CL_0	θ_1	θ_2	θ_3	θ_4	ΔOF°
Eq. 5[b]	*CYP2B6/CYP2A6*	$CL = CL_0 + \theta_1 I_{01} + \theta_2 I_{02} + \theta_1 I_{10} + \theta_2 I_{11} + \theta_3 I_{12} + \theta_1 I_{20} + \theta_2 I_{21} + \theta_3 I_{22} + \theta_1 I_{30} + \theta_2 I_{31} + \theta_3 I_{32}$	1.8	2.59 7.42 9.74 14.6	3.15 11.6 11.9 19.6	10.9 14.3 18.8		−16
Eq. 6	*CYP2B6/CYP2A6*	*CYP2B6* $CYP2A6 \cdot \sqrt{q}$	1.75	8.15 0.95	2.42	9.21 3.44	19.3 2.49	−17
Eq. 7	*CYP2B6/CYP2A6*	*CYP2B6* $CYP2A6 \cdot \sqrt{q}$		2.02 1.21	7.7	9.45	13.6	−16
Eq. 8	*CYP2B6/CYP2A6*	$CYP2B6 \cdot \sqrt{p}$ $CYP2A6 \cdot \sqrt{q}$	1.5	7.7 1.2				−12
Eq. 5[b]	*CYP2B6/CYP3A4* _rs4646437	$CL = CL_0 + \theta_1 I_{01} + \theta_2 I_{02} + \theta_1 I_{10} + \theta_2 I_{11} + \theta_3 I_{12} + \theta_1 I_{20} + \theta_2 I_{21} + \theta_3 I_{22} + \theta_1 I_{30} + \theta_2 I_{31} + \theta_3 I_{32}$	1.66	2.46 10.5 13.3 16.3	3.9 11 12.3 17.0	10.6 13.5 19.3		−25
Eq. 6	*CYP2B6/CYP3A4* _rs4646437	*CYP2B6* $CYP3A4\_rs \cdot \sqrt{r}$		1.6 1.4	10.7 0.1	11.2 1.6	15.3 2.6	−22
Eq. 7	*CYP2B6/CYP3A4* _rs4646437	*CYP2B6* $CYP3A4\_rs \cdot \sqrt{r}$		1.62 1.36	8.99	11.5	16.9	−22
Eq. 8	*CYP2B6/CYP3A4* _rs4646437	$CYP2B6 \cdot \sqrt{p}$ $CYP3A4\_rs \cdot \sqrt{r}$	1.62	7.3 1.34				−18
Eq. 5[b]	*CYP2B6/CYP3A4*1B*	$CL = CL_0 + \theta_1 I_{01} + \theta_2 I_{02} + \theta_1 I_{10} + \theta_2 I_{11} + \theta_3 I_{12} + \theta_1 I_{20} + \theta_2 I_{21} + \theta_3 I_{22} + \theta_1 I_{30} + \theta_2 I_{31} + \theta_3 I_{32}$	1.69	2.33 10.6 13.4 16.4	3.23 10.3 11.7 17.2	10.8 13.6 19.4		−14
Eq. 6	*CYP2B6/CYP3A4*1B*	*CYP2B6* $CYP3A4*1B \cdot \sqrt{s}$		1.64 1.1	10.7 0.4	11.2 1.2	15.3 2.7	−13
Eq. 7	*CYP2B6/CYP3A4*1B*	*CYP2B6* $CYP3A4*1B \cdot \sqrt{s}$		1.62 1.1	8.99	11.5	16.9	−12
Eq. 8	*CYP2B6/CYP3A4*1B*	$CYP2B6 \cdot \sqrt{p}$ $CYP3A4*1B \cdot \sqrt{s}$	1.65	7.6 1.1				−9
Eq. 5[b]	*CYP2B6/CYP3A5*	$CL = CL_0 + \theta_1 I_{01} + \theta_2 I_{02} + \theta_1 I_{10} + \theta_2 I_{11} + \theta_3 I_{12} + \theta_1 I_{20} + \theta_2 I_{21} + \theta_3 I_{22} + \theta_1 I_{30} + \theta_2 I_{31} + \theta_3 I_{32}$	1.45	2.22 6.0 13.4 16.5	3.25 11.6 11.9 17.0	10.6 13.6 19.2		−16
Eq. 6	*CYP2B6/CYP3A5*	*CYP2B6* $CYP3A5 \cdot \sqrt{t}$		1.38 1.1	10.7 0.1	11 1.8	15 2.4	−14
Eq. 7	*CYP2B6/CYP3A5*	*CYP2B6* $CYP3A5 \cdot \sqrt{t}$		1.4 1.22	9.1	11.7	17.1	−13
Eq. 8	*CYP2B6/CYP3A5*	$CYP2B6 \cdot \sqrt{p}$ $CYP3A5 \cdot \sqrt{t}$	1.4	7.6 1.22				−10

ΔOF, difference in the objective function, compared to the final model structural model; ΔOF°, difference in the objective function compared to the model including CYP2B6 solely; ARV, antiretroviral medication; NRTI, non-nucleoside/nucleotide reverse transcriptase inhibitors; *n*, *p*, *q*, *r*, *s*, numbers of functional alleles (0 = Hom-LOF, 1 = Het-LOF, 2 = Hom-Ref, 3 = Het-GOF); NS, not statistically significant; PI, protease inhibitors.

[a]Differences in objective function compared to the rich model (Eq. 1). [b]I_{xy} represents the number of functional alleles for the x/y cytochromes. For clarity, θ have been numbered from 1 to 4. **P* < 0.05, ***P* < 0.01.

for **1B*, −18 for rs_4646437). No factor accounting for more than an additive interaction was observed (ΔOF = 0.0).

The joint assignment of *CYP2B6* and *CYP3A5* on CL also improved the fit as compared to *CYP2B6* alone (Eq. 5, ΔOF = −16). The successive nesting of models using functional scores successfully followed the paradigm previously described for other *CYPs*. The influence of *CYP3A5* on *CYP2B6* was appropriately described using Eqs. 6 or 7 (ΔOF >−13) or as a square root additive model (Eq. 8, ΔOF >−10). Again, an interaction between the two genes was not significant (ΔOF = 0.0).

A final joint model characterizing the cumulative influence of all the genetic variants on EFV CL was tested on the basis of the two-by-two combinations of genetic effects. The richest model that integrated the effects of all CYP alleles, using a generalization of Eqs. 6 and 7, improved the fit (ΔOF >−29 as compared to *CYP2B6* alone), but the impact of *CYP3A4*1B* and *CYP3A5* did not remain significant (ΔOF = 0.0 as compared to the rich model without those two alleles). The final model employed a single parameter estimate to quantify the influence of each of the alleles, *CYP2B6*, *CYP2A6*, and *CYP3A4* _rs4646437, using additive square root functions, which fitted the data appropriately (Eq. 10, ΔOF = −24). All models specified with proportional rather than additive effects gave very similar results (ΔOF <−0.5). In addition to genetic influences on CL, the influence of body weight remained the only significant demographic covariate (ΔOF = 19.2), while any ethnic influence vanished completely.

The final model estimated an average CL of 1.3 l/h in individuals carrying Hom-LOF *CYP2B6*, *CYP2A6*, and *CYP3A4_*rs4646437, which increased by 7.3, 0.7, and 1.03 l/h for the first active allele of those genes, respectively, and by another 0.41 times those factors for the second allele (where $0.41 = \sqrt{2} - 1$), with an additional 70% increase in CL associated with doubling of body weight. A summary of the model building procedure is presented in **Table 2** and the final population estimates in **Table 3.** A plot of the model-predicted concentration profile stratified by *CYP2B6* is shown in **Figure 2**. **Figure 3** represents the individual *post hoc* CL estimates with population average predictions for the different allelic combinations encountered.

Based on our final model, simulations show that, with the standard regimen of 600 mg of EFV daily, average trough concentrations are 1.19 (90% prediction interval: 0.6–2.35), 1.6 (0.8–2.5), and 8.1 mg/l (4.5–14.5) in *CYP2B6* Hom-Ref, Het-LOF, and Hom-LOF carriers, respectively, and 0.5 mg/l (0.2–1.0) in *CYP2B6* Het-GOF carriers. Taking into account the interindividual variability leads to the suggestion that most *CYP2B6* Hom-LOF individuals will exhibit concentrations exceeding the 1–4 mg/l range that is generally considered acceptable, and most individuals carrying a Het-GOF will have concentrations <1 mg/l. Predicted concentrations of 2.7 mg/ml (1.5–4.9) would be expected at a dosage regimen of 200 mg/day in *CYP2B6* Hom-LOF carriers. However, individuals having Hom-LOF of *CYP2A6*/*CYP3A4_* rs3434367 and *CYP2B6* will be exposed to considerably higher drug levels, yielding average predicted concentrations of 6.2 mg/ml (3.5–11.0) with a regimen of 200 mg/day.

Table 3 Final population pharmacokinetic parameter estimates of EFV

	Population mean		Interindividual variability	
Parameter	Estimate	SE (%)[a]	Estimate (%)[b]	SE (%)[c]
CL/F (l/h)[d]	1.3	18	27.8	43.8
θ_{2B6}[e]	7.3	7		
θ_{2A6}[e]	0.7	36		
$\theta_{3A4\_rs4646437}$[e]	1.03	27		
θ_{BW}[f]	0.7	42		
V_d/F (l)	332	16		
k_a (h^{-1})	0.6	38		
σ (CV%)[g]	30.8	44.2		

CL/F, mean apparent clearance; F, bioavailability; k_a, mean absorption rate constant; V_d/F, mean apparent volume of distribution.

[a]SEs of the estimates (SEE), defined as SE/estimate and expressed as percentages. [b]Estimate of variability is expressed as coefficient of variation (CV) (%). [c]SEs of the CV, taken as $\sqrt{(SE/estimate)}$ and expressed as percentage. [d]CL value in patients with Hom-LOF for *CYP2B6*, *CYP2A6,* and *CYP3A4_* rs4646437. [e]Contribution of *CYP2B6*, *CYP2A6,* and *CYP3A4* _rs4646437 to efavirenz (EFV) CL multiplied by $\sqrt{n}$ where $n = 0, 1, 2, 3$ for *CYP2A6,* $n = 0, 1, 2$ for *CYP2A6* and *CYP3A4* _rs4646437 (see text). [f]Relative influence of body weight on EFV clearance (see text). [g]Residual intrapatient variability, expressed as a CV (%).

DISCUSSION

This study enabled us to characterize and quantify for the first time the conjugated effects of major and minor metabolic pathways and their genetic variants on EFV pharmacokinetics in a population of HIV-1-infected patients. The average CL and variability of EFV plasma concentrations are in the range of values reported previously.[1–3] Among nongenetic covariates, we observed an impact of body weight on CL, as reported by others.[16–20] In our study, no differences could be observed between data from male and female subjects, but conflicting results exist in the literature.[20–23] The well-known influence of black ethnicity, which has been associated with *CYP2B6* and *CYP3A4* heterogeneity,[24,25] could

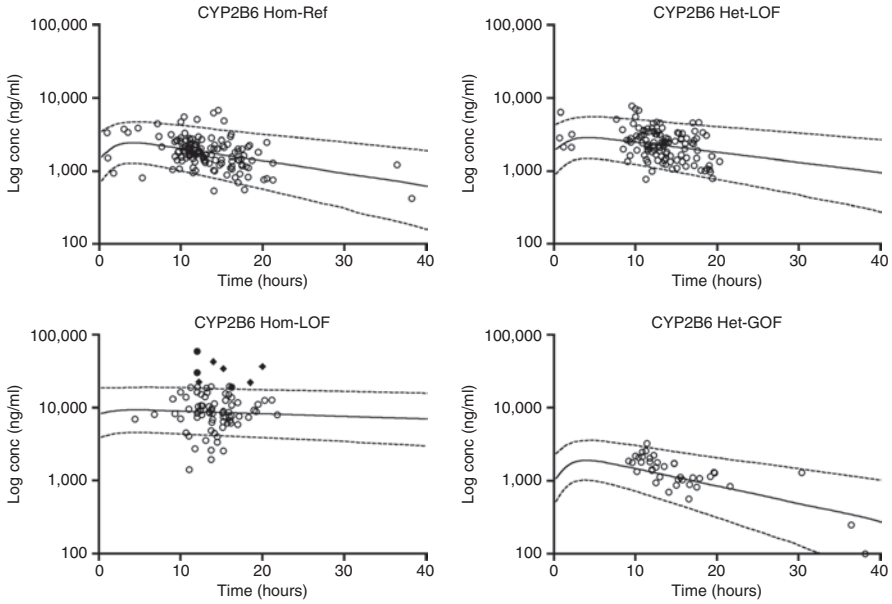

Figure 2 Efavirenz (EFV) plasma concentrations ($n = 393$) in 169 type I human immunodeficiency virus (HIV-1) individuals (open circles) in relation to *CYP2B6* polymorphism. Population predictions of the corresponding genotype are represented by black lines, and the 90% prediction interval is shown by gray dotted lines. Left lower panel: filled circles represent concentrations in individuals who are Hom-LOF for CYP2B6, CYP2A6, and CYP3A4_rs46464337, and filled diamonds represent concentrations in individuals who are Hom-LOF for CYP2B6 and Het-LOF for CYP3A4_rs4646437. Het, heterozygous; Hom, homozygous; LOF, loss of function.

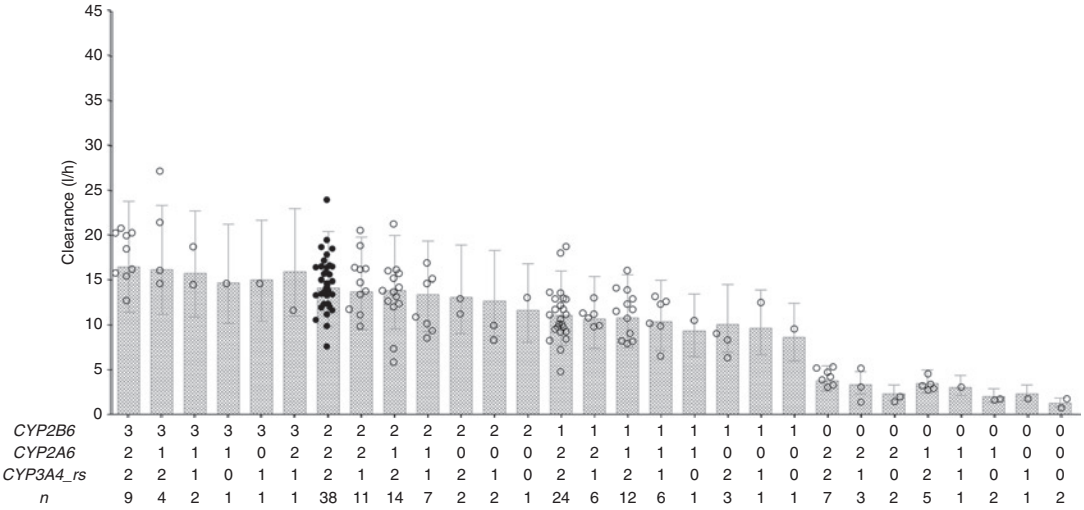

Figure 3 Individual predicted Bayesian clearances (open circles, the black circles correspond to individuals with reference alleles for all three cytochromes) and average predicted clearances (bars) with 90% population prediction interval for each *CYP2B6, CYP2A6*, and *CYP3A4* _rs4646437 allelic combination (according to score A categorization: 0 Hom-LOF/DOF, 1 Het-LOF/DOF, 2 Hom-Ref, and 3 Het-GOF; see text); *n* = number of individuals carrying the allelic combination (*n* = 0 for the eight combinations that are not represented). DOF, diminished function; GOF, gain of function; Het, heterozygous; Hom, homozygous; LOF, loss of function; Ref, reference allele.

be mostly explained by the joint influence of *CYP2B6*, *CYP2A6*, and *CYP3A4* variations, whereas its influence remained discernible when these *CYP* alleles were considered separately. Given the limited number of Hispanic ($n = 6$) and Asian ($n = 5$) individuals in our study, no clear effect on EFV levels could be attributed to these ethnic groups, although an influence has been reported previously.[1,3,10,20] Among genetic covariates, *CYP2B6* allelic variation accounted for most of the interindividual differences in EFV CL. The *CYP2A6* and *CYP3A4/A5* accessory pathways appeared to influence EFV elimination independent of *CYP2B6*. Among those, the overall impact of *CYP3A4_* rs4646437 was the largest; it accounted for 6% of CL variability. The unexpected lower CL in *CYP3A5* Hom-Ref carriers as compared to Hom-LOF carriers can be explained by the linked Hom/Het-LOF of *CYP2B6* and *CYP3A4_* rs4343437 observed in most individuals. This hypothesis is further confirmed by the lack of effect of *CYP3A5* when the influence of all cytochromes is assessed in a joint analysis. When information on *CYP2B6* was included along with *CYP2A6* and *CYP3A4* in joint analyses, an additive effect of accessory pathways was still present, both on fully functional *CYP2B6* and in the presence of reduced-function or gain-of-function alleles. However, the compensation ensured by these *CYP* alleles was small (1–2 l/h) and therefore more discernible on *CYP2B6* Hom-LOF. An evaluation of *CYP* genetic variations according to an activity score, as recently proposed by Gaedigk *et al.*[26] for *CYP2D6*, enabled us to quantify genetic influences of all alleles based on the same paradigm. A model of remarkable parsimony, which included only one parameter per allele and required no interaction term, could capture the nonlinear relationship between CL and the different genotypic groups. The use of such square root relationships in gene–dose effects was not described for other *CYP* isoenzymes, in particular for the noninducible CYP2D6,[24] which tend more toward linear effects.[27] This phenomenon suggests adaptive mechanisms that might be explained by the upregulation of extensive metabolizer alleles in response to an increase in concentration, possibly through the activation of nuclear receptors.[28,29] It is noteworthy that a similar pattern has already been reported for *CYP2B6*, not only in relation to EFV[30] but also in relation to S-methadone.[31] The use of different functional score classifications to implement partial activity levels failed to improve the model when compared with the traditional classification. The mechanisms by which allelic variants express a loss/diminished function could therefore not be translated in a "semiquantitative gene–dose system," as described by Steimer *et al.*[32] for amitriptyline and nortriptyline.

The cumulative influence of *CYP2B6*, *CYP2A6*, and *CYP3A4* _rs4646437 allelic variants on CL implies a critical 90% decrease of EFV elimination in triple-Hom-LOF individuals, in whom CL appeared reduced to 1.3 l/h as compared to the estimated 12.9 l/h in triple-Hom-Ref individuals. Of note, the only individual who exhibited extremely high EFV concentrations[33] was found to be triple-Hom-LOF; this emphasizes the importance of accessory pathways in EFV elimination. The interindividual variability in CL dropped from 65 to 27% in the final model, with *CYP2B6* genetic variants accounting for 31% and another 7% being explained by *CYP2A6, CYP3A4_* rs4646437, and body weight variations. The remaining variability might be attributed to adherence issues[34] or to variation in uridine-glucuronyltransferase metabolic pathways.

In conclusion, functional alleles of *CYP2B6* accounted for the major part of EFV interindividual variability. Genetic variations in EFV accessory metabolic pathways demonstrated their importance in EFV pharmacokinetics in addition to *CYP2B6*, in particular in individuals with limited *CYP2B6* function. The dosage is required to be reduced to 200 mg/day of EFV in individuals with impaired *CYP2B6* function so as to ensure drug levels within the therapeutic range. The expression of pharmacogenetic influences on EFV elimination could be characterized using a single common paradigm across all *CYPs*. This paradigm involves the addition of the contribution of each enzymatic pathway proportional to the square root of the number of

Table 4 Demographic and genetic characteristic of the population study

Characteristics	Value	% Of study population
Sex (no.)		
Men	124	73
Women	45	27
Age (years)		
Median (range)	47 (30–73)	—
Body weight (kg)		
Median (range)	77.5 (44–101)	—
Height (cm)		
Median (range)	179 (153–193)	—
Ethnicity (no.)		
White	142	83
Black	16	10
Hispanic	6	4
Asian	5	3
PIs (no.)		
Ritonavir	20	13
Saquinavir	4	3
Amprenavir	0	0
Lopinavir	15	9
Atazanavir	18	11
NRTIs (no.)		
Lamivudine	116	72
Stavudine	15	9
Didanosine	29	18
Abacavir	0	0
Tenofovir	29	18
Emtricitabine	4	2
Zidovudine	81	50
Entry inhibitors (no.)		
Enfuvirtide	4	2
CYP P450 inducers (no.)	2	1
CYP P450 inhibitors (no.)	4	2
CYP2B6 *genetic polymorphism (no.)*		
Hom-Ref	75	44
Het-LOF	53	33
Hom-LOF	23	14
Het-GOF	16	9
Het-LOF/Het-GOF[a]	2	1
CYP2A6 *genetic polymorphism (no.)*		
Hom-Ref	99	61
Het-LOF	55	30
Hom-LOF	13	8
Het-GOF	2	1
CYP3A4 *genetic polymorphism (no.)*		
Hom-Ref	138	82
Het-LOF *1B	24	14
Hom-LOF *1B	7	4
CYP3A4 *genetic polymorphism (no.)*		
Hom-Ref	118	70
Het-LOF_rs4646437	41	24
Hom-LOF_rs4646437	10	6
CY3A5 *genetic polymorphism (no.)*		
Hom-Ref	5	3
Het-LOF	30	18
Hom-LOF	134	79

GOF, gain of function; Het, heterozygous; Hom, homozygous; LOF, loss of function; NNRTIs, non-nucleoside reverse transcriptase inhibitors; NRTIs, nucleoside reverse transcriptase inhibitors; PIs, protease inhibitors; Ref, reference allele.

[a]Two individuals are LOF/GOF for *CYP2B6* and were considered to be Het-LOF.

functional alleles. Such a model appropriately predicts average CL for various allele combinations, and its mechanistic explanation warrants further investigation.

METHODS

Study population. A total of 169 HIV-1-infected individuals from the Swiss HIV Cohort Study were characterized with respect to *CYP2B6*, *CYP2A6*, and *CYP3A4/A5* genetic variations. EFV drug levels were measured during routine therapeutic drug monitoring according to local treatment guidelines. All participants gave their informed consent for genetic testing. A median of 1 concentration sample per individual (range 1–23) was collected between 0.6 and 38 h after the last drug intake under steady-state conditions.

Method of analysis. Blood samples (5 ml) were collected into lithium heparin or EDTA-K Monovette syringes (Sarstedt, Nümbrecht, Germany). Plasma was isolated by centrifugation, inactivated for virus at 60 °C for 60 min, and stored at −20 °C until analysis. Plasma EFV levels were determined by liquid chromatography coupled with tandem mass spectrometry in accordance with a validated method. The calibration curves were found to be linear up to 10 μg/ml, with a lower limit of quantification of 0.1 μg/ml.

Nomenclature and functional score. Alleles are designated in concordance with the *CYP* Allele Nomenclature Committee (http://www.cypalleles.ki.se). Proposed functional consequences for EFV pharmacokinetics have been reported for *CYP2B6*,[15] *CYP2A6*, and *CYP3A4/A5*.[35] The study participants were categorized into genotypic groups on the basis of the number of functional alleles (**Table 1**). The simplest scoring scheme (score A) assigned values of 2, 0, and 1 to the fully functional reference (Hom-Ref), homozygous (Hom-LOF), and heterozygous (Het-LOF) diminished/loss of function, respectively, and a value of 3 to *CYP2B6* gain-of-function alleles (Het-GOF). Two individuals having a single-gene duplication of *CYP2A6* were assimilated to the Hom-Ref group because they constituted only a small number. The classification was refined to distinguish between individuals with *CYP2B6* and *CYP2A6* loss/diminished function alleles, to reflect the predicted level of activity from *in vitro* studies (**Table 1**, scores B/C).

Pharmacokinetic structural model. EFV pharmacokinetics were characterized using a one-compartment model, as assessed previously.[2] Since EFV is administered only orally, CL and *V* represent apparent values.

Covariate model. The analyses of the covariate effects on CL were divided into three main sections for assessing: (i) the influence of demographic variables and concomitant medications, (ii) the impact of *CYP2B6*, *CYP2A6, CYP3A4*, and *CYP3A5* alleles based on univariate analyses, and (iii) the joint effect of *CYP2B6* with *CYP2A6, CYP3A4*, and *CYP3A5* alleles in multivariate analyses.

Demographic analyses. The typical value of CL was modeled to depend linearly on a covariate X (body weight, centered on the mean; categorical covariates coded as 0/1) as shown in the equation: $CL = \theta_a \cdot (1 + \theta_b \cdot X)$, where θ_a is the average estimate and θ_b is the relative deviation (positive or negative) from average attributed to the covariate X. The available demographic covariates were sex, ethnicity, age, body weight, and height. Only a few co-medications were recorded, and these were principally other antiretroviral drugs and known *CYP* inducers or inhibitors (**Table 4**).

Univariate genotype. In these analyses, each genotype was entered solo into the model. Several models relating CL with functional scores were tested using different methods (**Figure 1**) and compared with the richest possible model, which assigned a separate fixed effect to each score level as follows:

$$CL = CL_0 + \theta_1 I_1 + \theta_2 I_2 + \theta_3 I_3 \quad (1)$$

$$CL = CL_0 \cdot (1 + \theta_1 I_1) \cdot (1 + \theta_2 I_2) \cdot (1 + \theta_3 I_3) \quad (1a)$$

where CL_0 is the typical value of CL in Hom-LOF individuals (Hom-Ref for *CYP3A5*), I_i is an indicator variable that takes the value of 1 if an individual carries the ith genotypic score (i.e., I_1: Het-LOF, I_2: Hom-Ref, and I_3: Het-GOF) and 0 otherwise, and θ_i is the absolute or fractional (Eqs. 1/1a) change in CL relative to the Hom-LOF group. The impact of functional alleles on EFV CL was further explored to distinguish the difference between the genotypic groups, using two reduced models in which the same genotyping group was assigned to Hom-Ref and Het-LOF or to Hom-Ref and Het-GOF carriers (reduced 1 and 2, **Figure 1**). Competing models attempted to account for gene effect as a function of the number of functional alleles (**Table 1**, score A), using linear and power relationships with either additive or proportional (data not shown) impact, using the following models:

$$CL = CL_0 + \theta_1 \cdot n \quad (2)$$

$$CL = CL_0 + \theta_1^n \quad (3)$$

$$CL = CL_0 + \theta_1 \sqrt{n} \quad (4)$$

where $n = 1$, 2, or 3 represents the functional score, and θ_1 the average contribution per active allele above that of Hom-LOF CL (CL_0). The alternative activity scores B/C for *CYP2B6* and *CYP2A6* were explored using parameter models in Eqs. 2, 3, or 4 and compared with an extension of the rich model (Eq. 1).

Gene–gene interaction analyses. The joint influence of functional alleles on EFV CL was first tested using pairwise conjunction of *CYP2B6* with each of the other *CYP* alleles, so as to finally build up a model including all genetic variants that have an influence. The investigation of the joint influence of *CYP2B6* and *CYP2A6* alleles is shown as an example. The richest model that served as reference for the evaluation of reduced competing models was:

$$CL = CL_0 + \theta_{01} I_{01} + \theta_{02} I_{02} + \theta_{10} I_{10} + \theta_{11} I_{11} + \theta_{12} I_{12} + \theta_{20} I_{20} + \theta_{21} I_{21} + \theta_{22} I_{22} + \theta_{30} I_{30} + \theta_{31} I_{31} + \theta_{32} I_{32} \quad (5)$$

where CL_0 is the Hom-LOF CL for both genes and I_{ij} is an indicator variable that takes the value of 1 for the *CYP2B6* ith/*CYP2A6* jth genotype carrier and is 0 otherwise, and each θ_{ij} estimates the absolute change in CL among the different genotypic groups. The same model was parameterized for relative changes (data not shown). The following competing models were evaluated:

$$CL = CL_0 + \theta_{0\_0} \cdot \sqrt{q} + \left(\theta_1 I_1 + \theta_{1\_1} \cdot \sqrt{q}\right) + \left(\theta_2 I_2 + \theta_{2\_2} \cdot \sqrt{q}\right) + \left(\theta_3 I_3 + \theta_{3\_3} \cdot \sqrt{q}\right) \quad (6)$$

$$CL = CL_0 + (\theta_1 I_1 + \theta_2 I_2 + \theta_3 I_3) + \theta_4 \cdot \sqrt{q} \quad (7)$$

$$CL = CL_0 + \theta_1 \cdot \sqrt{p} + \theta_2 \cdot \sqrt{q} \quad (8)$$

$$CL = CL_0 + \theta_1 \cdot \sqrt{p} + \theta_2 \cdot \sqrt{q} + \theta_3 \cdot (p \cdot q) \quad (9)$$

where p indicates the functional score for *CYP2B6* and q the score for *CYP2A6*. In Eq. 6, the contribution of *CYP2A6* (θ_{0_0},...,θ_{3_3}) is investigated on *CYP2B6* stratified by genotypic groups; in Eq. 7 the influence of *CYP2A6* is characterized using a single fixed-effect parameter θ_4 across all *CYP2B6* genotypes; and in Eq. 8 square root functions are integrated for both genes. Finally, an interaction term was allowed so as to further check for some nonadditive interaction between *CYP* variants (Eq. 9). All these models used either additive or proportional (data not shown) effects.

All significant allelic groups were integrated into a final model, wherein the contribution of each genotypic group was estimated using a generalization of Eqs. 6–8 to be finally formulated using the following additive or proportional (data not shown) relationships:

$$CL = CL_0 + \theta_1 \cdot \sqrt{p} + \theta_2 \cdot \sqrt{q} + \theta_3 \cdot \sqrt{r} + \theta_4 \cdot \sqrt{s} + \theta_5 \cdot \sqrt{t} \quad (10)$$

where CL_0 is the Hom-LOF CL for all genes and θ_i values estimate the absolute or fractional change in CL as a function of score A for different combinations of *CYP2B6* (p), *CYP2A6* (q), *CYP3A4* _rs4646437 (r), *CYP3A4*1B* (s), and *CYP3A5* (t) alleles.

Variance model. The individual CL values were modeled assuming a log-normal distribution (mean zero and variance Ω). A proportional error model (mean zero and variance σ^2) was used the description of intraindividual variability.

Parameter estimation and selection. NONMEM (version VI; NM-TRAN, version II, GloboMax, Hanover, MD) was used with FOCE INTERACTION to fit the models.[36] As goodness-of-fit statistics, NONMEM uses the objective function, which is approximately equal to minus twice the logarithm of the maximum likelihood. The likelihood ratio test, based on the reduction in objective function (ΔOF), was used to carry out comparisons between any two models. A ΔOF (−2 log likelihood, approximate χ^2 distribution) of 3.84, 5.99, and 7.81 points for 1, 2, or 3 additional parameters, respectively, was used for determining statistical significance ($P < 0.05$) of the difference between two models. The reliability of the results was checked on diagnostic goodness-of-fit plots, along with the measure of the SEs. The identification of potential outlier values resulting from compliance issues or inadequacy in self-reporting information was explored using a sensitivity analysis. One individual had an EFV concentration of 59,400 ng/ml, and this value was at first excluded to prevent single outlier effect but was integrated at the end. Except for this, all data were considered reliable. Simulations based on the final pharmacokinetic estimates were performed with NONMEM using 1,000 individuals to calculate the 90% prediction intervals. The concentrations encompassing the range from 5th to 95th percentile at each time point were retrieved in order to construct the intervals. Further simulations were performed for a series of genotype combinations in 1,000 individuals undergoing various dosage regimens (200, 400, 600, and 800 mg), so as to suggest the dosages that would ensure trough levels falling within the 1–4 mg/ml therapeutic interval in 90% of the individuals. The figures were generated using GraphPad Prism (version 4.00 for Windows; GraphPad Software, San Diego, CA, http://www.graphpad.com).

ACKNOWLEDGMENTS

M.A.-A. contributed to the pharmacokinetic modeling and J.D.I. to the genetic testing.

CONFLICT OF INTEREST

The authors declared no conflict of interest.

1. Barrett, J.S., Joshi, A.S., Chai, M., Ludden, T.M., Fiske, W.D. & Pieniaszek, H.J. Jr. Population pharmacokinetic meta-analysis with efavirenz. *Int. J. Clin. Pharmacol. Ther.* **40**, 507–519 (2002).
2. Csajka, C. *et al*. Population pharmacokinetics and effects of efavirenz in patients with human immunodeficiency virus infection. *Clin. Pharmacol. Ther.* **73**, 20–30 (2003).
3. Kappelhoff, B.S. *et al*. Population pharmacokinetics of efavirenz in an unselected cohort of HIV-1-infected individuals. *Clin. Pharmacokinet.* **44**, 849–861 (2005).
4. Marzolini, C., Telenti, A., Decosterd, L.A., Greub, G., Biollaz, J. & Buclin, T. Efavirenz plasma levels can predict treatment failure and central nervous system side effects in HIV-1-infected patients. *AIDS* **15**, 71–75 (2001).
5. Rotger, M. *et al*. Influence of CYP2B6 polymorphism on plasma and intracellular concentrations and toxicity of efavirenz and nevirapine in HIV-infected patients. *Pharmacogenet. Genomics* **15**, 1–5 (2005).
6. Haas, D.W. *et al*. Pharmacogenetics of efavirenz and central nervous system side effects: an Adult AIDS Clinical Trials Group study. *AIDS* **18**, 2391–2400 (2004).
7. Desta, Z. *et al*. Impact of CYP2B6 polymorphism on hepatic efavirenz metabolism in vitro. *Pharmacogenomics* **8**, 547–558 (2007).
8. Ward, B.A., Gorski, J.C., Jones, D.R., Hall, S.D., Flockhart, D.A. & Desta, Z. The cytochrome P450 2B6 (CYP2B6) is the main catalyst of efavirenz primary and secondary metabolism: implication for HIV/AIDS therapy and utility of efavirenz as a substrate marker of CYP2B6 catalytic activity. *J. Pharmacol. Exp. Ther.* **306**, 287–300 (2003).
9. Mutlib, A.E. *et al*. Identification and characterization of efavirenz metabolites by liquid chromatography/mass spectrometry and high field NMR: species differences in the metabolism of efavirenz. *Drug Metab. Dispos.* **27**, 1319–1333 (1999).
10. Cressey, T.R. & Lallemant, M. Pharmacogenetics of antiretroviral drugs for the treatment of HIV-infected patients: an update. *Infect. Genet. Evol.* **7**, 333–342 (2007).
11. Klein, K. *et al*. Genetic variability of CYP2B6 in populations of African and Asian origin: allele frequencies, novel functional variants, and possible implications for anti-HIV therapy with efavirenz. *Pharmacogenet. Genomics* **15**, 861–873 (2005).
12. Wyen, C. *et al*. Impact of CYP2B6 983T>C polymorphism on non-nucleoside reverse transcriptase inhibitor plasma concentrations in HIV-infected patients. *J. Antimicrob. Chemother.* **61**, 914–918 (2008).
13. Wang, J. *et al*. Identification of a novel specific CYP2B6 allele in Africans causing impaired metabolism of the HIV drug efavirenz. *Pharmacogenet. Genomics* **16**, 191–198 (2006).
14. Tsuchiya, K. *et al*. Homozygous CYP2B6 *6 (Q172H and K262R) correlates with high plasma efavirenz concentrations in HIV-1 patients treated with standard efavirenz-containing regimens. *Biochem. Biophys. Res. Commun.* **319**, 1322–1326 (2004).
15. Rotger, M. *et al*. Predictive value of known and novel alleles of CYP2B6 for efavirenz plasma concentrations in HIV-infected individuals. *Clin. Pharmacol. Ther.* **81**, 557–566 (2007).
16. Ofotokun, I., Chuck, S.K. & Hitti, J.E. Antiretroviral pharmacokinetic profile: a review of sex differences. *Gend. Med.* **4**, 106–119 (2007).
17. Hitti, J. *et al*. Sex and weight as covariates in the pharmacokinetics of efavirenz, indinavir, and nelfinavir. Program and Abstract of the 11th Conference on Retroviruses and Opportunistic Infections, San Francisco, CA, 8–11 February 2004. Abstract no. 604.
18. López-Cortés, L.F. *et al*. Pharmacokinetic interactions between efavirenz and rifampicin in HIV-infected patients with tuberculosis. *Clin. Pharmacokinet.* **41**, 681–690 (2002).
19. Matteelli, A. *et al*. Multiple-dose pharmacokinetics of efavirenz with and without the use of rifampicin in HIV-positive patients. *Curr. HIV Res.* **5**, 349–353 (2007).
20. Pfister, M. *et al*. Population pharmacokinetics and pharmacodynamics of efavirenz, nelfinavir, and indinavir: Adult AIDS Clinical Trial Group Study 398. *Antimicrob. Agents Chemother.* **47**, 130–137 (2003).
21. Burger, D. *et al*. Interpatient variability in the pharmacokinetics of the HIV non-nucleoside reverse transcriptase inhibitor efavirenz: the effect of gender, race, and CYP2B6 polymorphism. *Br. J. Clin. Pharmacol.* **61**, 148–154 (2006).
22. Rotger, M., Csajka, C. & Telenti, A. Genetic, ethnic, and gender differences in the pharmacokinetics of antiretroviral agents. *Curr. HIV/AIDS Rep.* **3**, 118–125 (2006).
23. Lamba, V. *et al*. Hepatic CYP2B6 expression: gender and ethnic differences and relationship to CYP2B6 genotype and CAR (constitutive androstane receptor) expression. *J. Pharmacol. Exp. Ther.* **307**, 906–922 (2003).
24. Ingelman-Sundberg, M., Sim, S.C., Gomez, A. & Rodriguez-Antona, C. Influence of cytochrome P450 polymorphisms on drug therapies: pharmacogenetic, pharmacoepigenetic and clinical aspects. *Pharmacol. Ther.* **116**, 496–526 (2007).
25. Lamba, J.K. *et al*. Common allelic variants of cytochrome P4503A4 and their prevalence in different populations. *Pharmacogenetics* **12**, 121–132 (2002).
26. Gaedigk, A., Simon, S.D., Pearce, R.E., Bradford, L.D., Kennedy, M.J. & Leeder, J.S. The CYP2D6 activity score: translating genotype information into a qualitative measure of phenotype. *Clin. Pharmacol. Ther.* **83**, 234–242 (2008).
27. Honda, M. *et al*. Multiple regression analysis of pharmacogenetic variability of carvedilol disposition in 54 healthy Japanese volunteers. *Biol. Pharm. Bull.* **29**, 772–778 (2006).
28. Faucette, S.R. *et al*. Relative activation of human pregnane X receptor versus constitutive androstane receptor defines distinct classes of CYP2B6 and CYP3A4 inducers. *J. Pharmacol. Exp. Ther.* **320**, 72–80 (2007).
29. Itoh, M. *et al*. Induction of human CYP2A6 is mediated by the pregnane X receptor with peroxisome proliferator-activated receptor-gamma coactivator 1alpha. *J. Pharmacol. Exp. Ther.* **319**, 693–702 (2006).
30. Nyakutira, C. *et al*. High prevalence of the CYP2B6 516G-->T(*6) variant and effect on the population pharmacokinetics of efavirenz in HIV/AIDS outpatients in Zimbabwe. *Eur. J. Clin. Pharmacol.* **64**, 357–365 (2008).
31. Crettol, S. *et al*. Methadone enantiomer plasma levels, CYP2B6, CYP2C19, and CYP2C9 genotypes, and response to treatment. *Clin. Pharmacol. Ther.* **78**, 593–604 (2005).
32. Steimer, W. *et al*. Allele-specific change of concentration and functional gene dose for the prediction of steady-state serum concentrations of amitriptyline and nortriptyline in CYP2C19 and CYP2D6 extensive and intermediate metabolizers. *Clin. Chem.* **50**, 1623–1633 (2004).
33. Hasse, B., Günthard, H.F., Bleiber, G. & Krause, M. Efavirenz intoxication due to slow hepatic metabolism. *Clin. Infect. Dis.* **40**, e22–e23 (2005).
34. Molto, J. *et al*. Variability in non-nucleoside reverse transcriptase and protease inhibitors concentrations among HIV-infected adults in routine clinical practice. *Br. J. Clin. Pharmacol.* **63**, 715–721 (2007).
35. Di Lulio, J. *et al*. *In-vivo* analysis of efavirenz metabolism in individuals with impaired CYP2A6 function. *Pharmacogenet. Genomics* (in press).
36. Beal, S.L., Sheiner, L.B. & Boeckmann, A.J. (eds.). NONMEM Users Guides, (1989–2006) (Icon Development Solutions, Ellicott City, MD, 2008).